Pseudo-stem banana fiber as a potential low-cost adsorbent to remove methylene blue from synthetic wastewater

Rahman, Md Wasikur

2022-10

Pseudo-stem banana fiber as a potential low-cost adsorbent to remove methylene blue from synthetic wastewater

Md. Wasikur Rahman[1] · Sumaya Tarannum Nipa[1] · Sarmin Zaman Rima[1] · Md. Mahmudul Hasan[1] ·
Raghunath Saha[1] · Md. Abdul Halim[2] · Yousuf Ali[1] · Anjan Deb[3]

Abstract

In this work, pseudo-stem banana *(Musa acuminata)* (PBF) fiber was utilized as a potential low-cost natural adsorbent to uptake methylene blue (MB) dye from synthetic wastewater by batch adsorption process. Different adsorption factors like contact time, pH, initial concentration, and adsorbent dosage were explored and found that the separation process is strongly pH dependent. Additionally, the adsorption data were fitted with various adsorption isotherms like Langmuir, Freundlich, Temkin, and Dubinin–Radhushkevich models to detect the adsorption equilibrium phenomena. Reaction kinetics was inspected using pseudo-first-order and second-order kinetic models. Mass transfer and intra-particle diffusion analyses indicate the adsorption mechanism of the system described particularly in the context. Furthermore, scanning electron spectroscopy (SEM) and Fourier transformed infrared spectroscopy (FTIR) were conducted to get the morphology and surface properties of the adsorbent, respectively. As a result, the as-prepared banana fiber can be proposed as a cheap suitable adsorbent to separate dyestuffs from industrial wastewater.

Keywords Adsorption · Banana fiber · Methylene blue · Isotherm · Kinetics · Mechanism

Introduction

Water is a very important part of human civilization; therefore, the contamination of water by industrial effluent is a great concern all over the world (Helmer et al. 1998; Lehr et al. 1980). To save water to save the world is the current slogan and to ensure a safer world for the future mankind is a great demand. The water crisis is increasing day by day. According to World Water Day, 2016 the water demand is increasing tremendously with the establishment of different industries, especially, heavy industries like textile, pharmaceuticals, leather, cosmetics, and agricultural sectors. Consequently, a huge amount of wastewater is generating from these industries and thronging them to the environmental water resources thus water pollution is occurring. It has been found that more than one lac types of dyes are commercially available and approximately 7×10^5 tons of wastewater is generated every year (Ozmen et al. 2008). Water can easily be polluted by dye molecules as a very small amount of dye can be detectable in open eyes (Robinson et al. 2001); therefore, discharged dyes are very harmful to the environment (Faur-brasquet et al. 2003). The dye is a mixture of various chemical compounds which used to color the fabric mainly in textile industries and cause serious water pollution whenever they are exposed to water (Garg et al. 2004). For example, methylene blue (MB) is commercially used as a dye, and water containing MB has many diverse effects on human, animals, and plants if they come in contact with each other. Therefore, the treatment of wastewater containing MB is an essential issue now a day. The existence of MB in environmental water resources affects the growth of plants as it hinders the photosynthetic rate in plants and it also origins various diseases in animals living in water kingdom (Taylor et al. 2015, 2013). Moreover, it causes many harmful diseases in the human body, for example, staining of skin, vomiting, nausea, bladder irritation, headache, fever,

✉ Md. Wasikur Rahman
   w.rahman@just.edu.bd; mwrahman.ump@gmail.com

1   Department of Chemical Engineering, Jashore University
    of Science and Technology, Jashore 7408, Bangladesh

2   Department of Chemistry, Jashore University of Science
    and Technology, Jashore 7408, Bangladesh

3   Department of Chemistry, School of Natural Science,
    University of Helsinki, Yliopistonkatu 4, 00100 Helsinki,
    Finland

hypertension, etc. (Mokhlesi et al. 2003; Harvey and Keitt 1983).

Many methods are well known for industrial wastewater treatment like solvent extraction (Muthuraman 2011), membrane separation process (Seader and Henley 2011), electrochemical process (Bessegato et al. 2014), biological treatment (Almeida and Corso 2014), activated carbon (Emilia et al. 2014), oxidation (Doumic et al. 2014), etc.; however, most of these processes are complex and costly. In contrast, the adsorption (chemical or physical) process (Adebayo et al. 2014) is a worldwide recognized method for wastewater treatment as it is simple, cost-effective, prospective, and the adsorbents are abundant globally (Prola et al. 2013; Chen et al. 2013). Various types of low cost and effective adsorbents such as *Mangifera indica* seeds (Alencar et al. 2012), *Nypa fruticans* (Ali et al. 2016), coconut leaves (Jawad et al. 2016), tea dust (Khan et al. 2016), orange peels (Ángel et al. 2016), sawdust (Ál-husseiny, H. A. 2014), water hyacinth (Alam et al. 2015), *Citrus limetta* peels (Shakoor and Nasar 2016), mushroom substrate (Yan and Wang 2013), sugarcane bagasse (Zhang et al. 2013), banana peels (Amel et al. 2012), potato peels (Guechi and Hamdaoui 2016), stone olives (Hemsas et al. 2014), maize stem (Vučurović et al. 2014), palm kernel fiber (El-Sayed, G. O. 2011), pea shell (Khan et al. 2014), date palm leaves (Gouamid et al. 2013), etc., have already been developed to remove dyestuffs from industrial wastewater. Numerous factors like adsorption capacity and applicability, availability, cost-effectiveness, etc., should be considered during adsorbent selection. Considering this issue, the banana plant is selected as a locally available and inexpensive adsorbent to uptake MB from wastewater. The banana plant is a plant of the *Musaceae* family and its scientific name is *Musa acuminate* (Calvert 1990). The basic properties of the PBF are displayed in Table 1.

In our recent study, the performance of the PBF adsorbent was investigated for the removal of MB from synthetic wastewater. Structural features of the adsorbent were studies and the process parameters were optimized. The equilibrium

data were analyzed with Langmuir, Freundlich, Temkin, and Dubinin–Radgushkevich isotherms to find out the adsorption mechanism. The reaction kinetics was determined by the pseudo-first-order and second-order kinetic models. Intraparticle diffusion and mass transfer analyses including the adsorption mechanism of the PBF/MB system were carried out in the context.

Materials and methods

Preparation of adsorbent

The adsorbent was prepared from low-cost and locally available materials. Banana fiber is a very cheap and locally available material and banana plants were collected from the local area of Jashore, Bangladesh. At first, the banana stems washed with DI water to separate dirt and unwanted parts. The clean stems are then cut into small pieces and wash again with DI water. The banana stem slices were then soaked for 40 min in a 40% solution of HCl and blended using a blender. The fiber was then separated by filtering the blended banana fiber. The filtered banana fiber was washed with DI water several times and dried at a certain temperature of 110 °C accordingly for 36 h. The as dried fiber was then ground and fine particles of 315–500 μm size were separated by using a sieve (Model: RETSCH, AS 200 Basic). The powder of the banana fiber was then stored in an air tight container to use as an adsorbent for the experiment.

Characterization of PBF adsorbent

Various techniques were carried out to analyze different characteristics of the PBF adsorbent. The functional groups of the adsorbent surface were detected by using an FTIR (FTIR 2000, Shimadzu, Kyoto, Japan). In this technique, approximately 2% of the sample was placed in 250 mg KBr disks to prepare the FTIR sample. The FTIR spectra were recorded in a range from 400 to 4000 cm^{-1} and with a resolution of 4 cm^{-1}. The recorded FTIR spectra reveal the functional group present on the adsorbent surface. Additionally, the morphology of the banana fiber surface was investigated by using a Leo 435 VP scanning electron microscope (SEM). The porosity of the banana fiber surface was produced by SEM images of various magnifications at 5 kV.

Preparation of stock solution

Methylene Blue of analytical grade was collected from Merck, Germany. Adsorbate solution was prepared by dissolving a calculated amount of MB dye in DI water. This solution was used as a stock solution and experimental solutions were prepared by diluting this solution. For making

Table 1 Basic properties of banana fiber (Ferdus Alam 2021)

Properties	Quantity
Tenacity	29.98 g/denier
Fineness	17.15
Moisture regain	13.00%
Elongation	6.54
Alcon-ben extractives	1.70%
Total cellulose	81.80%
α cellulose	61.50%
Residual gum	41.90%
Lignin	15.00%

the experiment at first 100 ml solution was prepared by dissolving 50 mg of MB in 500 ml of DI water. Additionally, solutions of different concentrations ranging from 25 to 300 were prepared for the experiment.

Batch adsorption study

Batch adsorption experiments were carried out to exemplify the adsorption performance of the PBF adsorbent to uptake the dye from synthetic wastewater at various operating conditions such as solution pH, initial dye concentration, and adsorbent dosage. The laboratory experiments were conducted at normal temperature and pressure. The required amount of adsorbents was taken in a conical flask containing as prepared 100 ml dye solution. The solution pH was adjusted by the inclusion of a calculated amount of 0.1 M NaOH or 0.1 M HCl. Afterward, 0.2 g of PBF was placed in the controlled pH solution and kept shaking for 12 h to reach the equilibrium. The adsorption was investigated using 100 ml of different dye concentrations (25–300 ppm) to understand the effect of solution concentration on adsorption. Additionally, the adsorption dosages effect was also examined by adding different dosages of PBF adsorbent (0.25–4.0 g) in 100 ml of dye solution of 100 ppm at constant pH 6 with a contact time of 12 h. The effect of contact time was determined by changing the time duration (10–300 min) of the adsorption process. In this process, 0.5 g of adsorbent was added in 100 ml of dye solution of 100 ppm at a pH 6. A UV visible spectrophotometer (HACH–DR–4000) was used at a wavelength of 666 nm to analyze the experimental solution after attaining the equilibrium concentration. The approximate dye removal percentage was computed using the given equation:

$$\text{MB Removal } \% = \frac{C_o - C_t}{C_o} \times 100\%$$

where, C_t is the concentration of the MB solution at time, t and C_o is the initial concentration of the dye solution. The quantity of dye adsorbed on the PBF adsorbent at equilibrium, q_e (mg/g) is computed by the equation given below:

$$q_e = \frac{(C_0 - C_e)V}{W}$$

where, C_e is the concentration of dye solution at equilibrium (mg/l), W is the mass (g) of dry adsorbent, and V is the volume (l) of the dye solution.

Adsorption isotherm study

The information about the distribution of adsorbate molecules on the surface of the adsorbent can be found by the adsorption isotherm study. Generally, adsorption isotherm helps to correlate dye adsorbate present in the aqueous solution and the adsorption capacity of the adsorbent. Adsorption was carried out on banana fiber adsorbent at different solution concentrations from 25 to 300 ppm keeping other parameters (adsorbent dosage 0.5 g, pH 6, solution volume 100 ml, contact time 12 h) constant. Additionally, different models of adsorption isotherm like Langmuir, Freundlich, Temkin, and Dubinin–Radushkevich were used to fit the adsorption data.

Langmuir isotherm

Langmuir adsorption isotherm model depicts that uniform adsorption occurs due to the homogenous distribution of energies through the surface and no transmigration takes place on the adsorbent surface amid adsorbates (Rotliwala et al. 2015). Langmuir adsorption isotherm equation can be expressed as follows:

$$q_e = \frac{Q_o K_L C_e}{1 + K_L C_e}$$

The linear form of the Langmuir adsorption isotherm equation is as follows:

$$\frac{1}{q_e} = \frac{1}{Q_0} + \frac{1}{Q_0 K_L C_e}$$

where, Q_o is the highest coverage of monolayer adsorption (mg/g), and K_L is the isotherm constant (l/mg).

By plotting $1/q_e$ versus $1/C_e$ a linear line was found; then the values of K_L and Q_o were calculated by the intercept and slope of the straight line. Langmuir isotherm model can be described in terms of a dimensionless constant, R_L which is known as separation factor can be express as follows:

$$R_L = \frac{1}{1 + (1 + K_L C_0)}$$

where, K_L represents the adsorption constant related to the energy of the adsorption. The value of R_L is very important for adsorption. If the R_L value is higher than one ($R_L > 1$), the adsorption is unfavorable. Similarly, if the R_L value is equal to one ($R_L = 1$), the adsorption likely to be linear; and if the value is less than one and higher than zero ($1 > R_L > 0$), the adsorption is favorable (Rotliwala et al. 2015).

Freundlich isotherm

Freundlich adsorption model supports to describe the characteristics of the heterogeneous surface. This model can be written as follows:

$$q_e = K_f (C_e)^{1/n}$$

where, n is the intensity of adsorption and K_f represents the isotherm constant (mg/g). The linear form of the isotherm model can be express as follows:

$$log\ q_e = log\ K_f + \frac{1}{n}\ log\ C_e$$

where, $1/n$ defines the strength of adsorption. If the value of $1/n$ is one ($1/n = 1$), the partition between the two-phases is independent of concentration. Similarly, if the value is less than one ($1/n·1$), it indicates normal adsorption and if the value is higher than one ($1/n·1$), then cooperative adsorption takes place (Indhumathi and Saraswathy 2011).

Temkin isotherm

The interaction among adsorbate/adsorbent can be illustrated by the Temkin isotherm model. The equation of the isotherm model can be expressed as follows:

$$q = \frac{RT}{b} \ln\left(k_T C_e\right)$$

The linear form of the above equation can be shown as follows:

$$q_e = B \ln k_T + B\ ln\ C_e$$

where, $B = (RT/b)$ is a constant associated with the heat of adsorption, R is the ideal gas constant (8.314 J/mol.K), b is a Temkin constant related to the heat of adsorption (kJ/mol), T is the temperature (K) and k_T implies the Temkin equilibrium constant which is related to the binding energy (Bhattacharya et al. 2008a).

Dubinin–Radushkevich isotherm

Dubinin–Radushkeyich isotherm is an additional model for the adsorption of dye molecules on the adsorbent surface. The equation for Dubinin–Radushkeyich can be expressed as follows:

$$q_e = q_s exp\left(-B\varepsilon^2\right)$$

where, ε can be defined by the following equation:

$$\varepsilon = RT \ln\left(1 + \frac{1}{C_e}\right)$$

where, B is the adsorption constant, E represents the mean free energy. The energy, E can be calculated by the following equation when the MB molecules adsorbed on the PBF adsorbent surface from the bulk of the solution:

$$E = \frac{1}{\sqrt{2B}}$$

Adsorption kinetics study

The adsorption kinetics of the process can be determined by a batch adsorption experiment. In this process calculated amount of adsorbent is added in a 100 ppm solution of MB. Whereas, the pH was maintained at 6 and the contact time changed from 10 to 300 min. The dye removal percentage was monitored after each batch experiment. The adsorption percentage was computed using the equation below:

$$q_e = \frac{(C_0 - C_e)V}{W}$$

where, the symbol q_e indicates the quantity of dye adsorbed at equilibrium, V is the volume of the dye solution, C_o is the initial solution concentration of dye and C_e is the dye solution concentration at equilibrium. W is the weight of the adsorbent in grams. Adsorption kinetics can be determined by using pseudo-first and second-order kinetics models.

Pseudo-first-order model

The adsorption rate constant can be measured by the pseudo-first-order kinetic model. The equation for the pseudo-first-order kinetic model is shown as (Bhattacharya et al. 2008a).

$$\log (q_e - q_t) = \log q_e - \frac{k_1}{2.303}t$$

where, q_e represents the quantity of dye adsorbed at equilibrium and q_t indicates the amount of adsorbate adsorbed after time t on the surface of the adsorbent. k_1 indicates the adsorption kinetics rate constant (min^{-1}). By plotting $log(q_{e-}\ q_t)$ versus t a linear line was found, the value of k_1 is determined from the slope of the linear line (Bhattacharya et al. 2008a).

Pseudo-second-order model

The kinetics data can be analyzed by a pseudo-second-order model. The adsorption capacity is proportionally related to the surface active sites of the adsorbent. The equation for the pseudo-second-order kinetics model can be written as (Ho et al. 2000).

$$\frac{t}{q_1} = \frac{1}{k_2 q_e^2} + \frac{1}{q_e}t$$

where, k_2 is the second-order kinetics constant. By plotting t/q_1 versus t, a straight line was obtained and the value of q_e and k_2 (g mg^{-1} min^{-1}) is obtained from the slope and intercept of the straight line.

Mass transfer analysis

The transfer of MB dye molecules (mass transfer) from the solution to the surface of the banana fiber powder was carried out by the equation of the Mckay et al. (1981),

$$\text{In} \frac{C_t}{C_0} - \frac{1}{1 + \text{MK}_{bq}} = \text{In} \frac{MK_{bq}}{1 + MK_{bq}} - \frac{1 + MK_{bq}}{MK_{bq}} \beta S_s t$$

Where, β is the mass transfer coefficient. The value of β is determined from the slope of the individual plots of $\{(1 + MK_{bq})/MK_{bq}\}\beta S_s$. Additionally, a graph was carried out by plotting $ln\{C_t/C_0 - 1/(1 + MK_{bq})\}$ versus t.

Intra-particle diffusion model

Various kinetics models were investigated, the interparticle diffusion model is the most important of them (Demirbas et al. 2004). The equation of Weber and Morris can be used to describe of interparticle diffusion mechanism (Weber and Carrell Morris 1963). The Weber and Morris rate equation can be expressed by the following equation:

$$K_{id} = q_t/t^{1/2}$$

where, K_{id} represents the rate constant for intra-particle diffusion (mg/g min$^{1/2}$). By plotting q_t versus $t^{1/2}$ a linear line is obtained the value of K_{id} can be measured from the slope of the straight line. If the line is not gone through the origin and the line is not linear then interparticle diffusion is not the only mechanism (Okoronkwo and Anwasi 2008). Interparticle diffusion was conducted in a 100 ml dye solution of 100 ppm where the contact time and pH of the solution were $t^{1/2}$ and 6, respectively.

Results

Adsorbent characterizations

FTIR study of the adsorbent

FTIR analysis of the banana (*Musa acuminata*) pseudo-stem is indicative of molecular functional groups which demonstrate important characteristics of the fiber presented in Fig. 1. Abraham et al. (Abraham et al. 2011) discovered the major constituents of the PBF to be cellulose, hemicellulose, and lignin which are composed of alkanes, alcohols, aromatic ketones, and esters with various functional groups containing oxygen. The work enables to identify the nature of the chemical linkages.
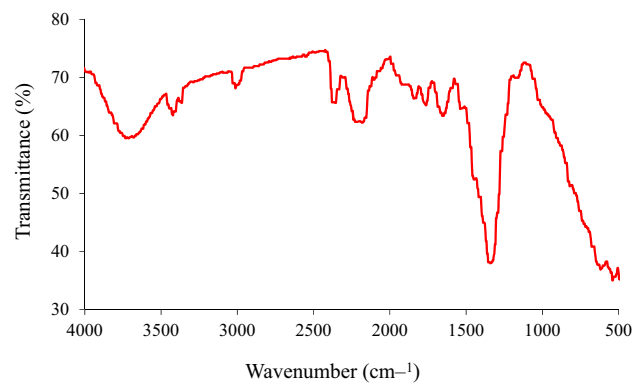

Fig. 1 FTIR spectrum of pseudo-stem banana fiber

The absorption bands at 3750 and 3430 cm^{-1} are due to O–H groups and stretching vibration of O–H bonding. Ibrahim et al. (Ibrahim et al. 2010) reported that O–H stretching is related to absorbed alcohols which are common for all the constituents of the fiber. The characteristics of any natural fiber can be explained by C–H stretching and the absorption band observed at 3032 cm^{-1} for the current study. Moreover, the bands at 2380 and 2230 cm^{-1} are associated with the molecular linkages of the PBF.

Besides, the bands at nearby 1780 and 1670 cm^{-1} are related to C=O stretching attributed to acetyl or ester groups of the cellulose constituents. The spectrum exhibited strong bands at 1355 and 1215 cm^{-1} are due to C–H deformation and lignin. In fact, C–H and C–O deformation stand for ether linkages (Ibrahim 2002). The band exposed at 1135 cm^{-1} is due to dialkyl ether linkages of C–O–C symmetric stretching and C–O stretching vibration present in the key components of the PBF. A broad region of overlapping bands of absorption (2000–1400 cm^{-1}) due to aromatic linkages of C–C, C=C, OH, CO, CH$_n$, C–O–C, C–H. These features are characteristics of β – glycosidic linkages amid the repeating units of anhydroglucose present in cellulose.

SEM analysis

Surface morphology and basic physical properties of the PBF material are merely characterized by SEM. The SEM image of the banana powder is presented in Fig. 2. The Figure revealed the morphology of the pristine banana fiber that displays rough surface and the average diameter of the pores (approximately 1 μm) results in the better possibility to be trapped and adsorbed waste materials into these pores.

The walls of the pores are composed of fibrils which are embedded in a uniform matrix (Lüttge et al. 1992). It has been proposed that fibrils are made of cellulose which constitutes the skeleton of cellular walls. They appeared rather in parallel arrangement point out the characteristics of the secondary wall of the plant (Fig. 2, inset) (Bilba et al. 2007).
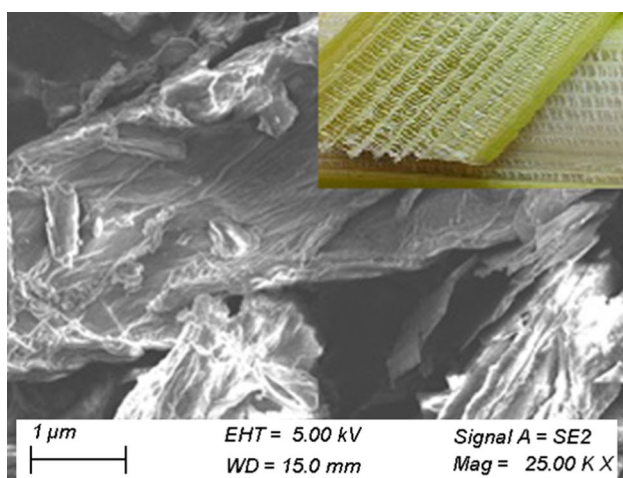
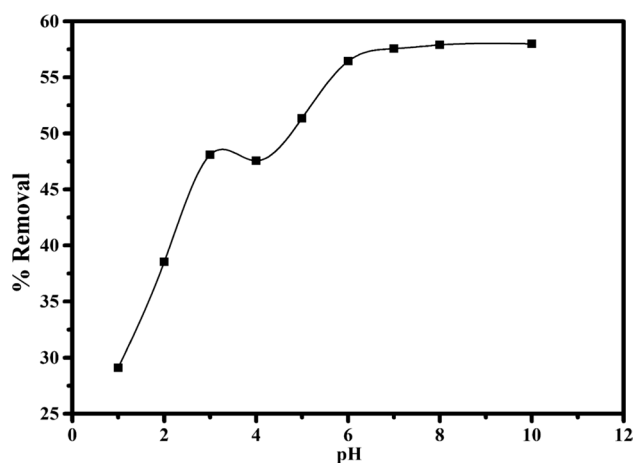**Fig. 2** SEM spectrum of pseudo-stem banana fiber and original banana fiber (inset)

Fig. 3 Impact of solution pH on MB dye adsorption on PBF adsorbent surface at optimum conditions (MB concentration 100 ppm, adsorbent dosage 0.2 g/l, contact time 12 h)

The homogenous matrix is conceivably a mixture of various lignin, polysaccharide acids, and hemicellulose as discoursed by FTIR.

Batch adsorption study

Effect of solution pH

pH is one of the most important parameters which affects the adsorption capacity of the adsorbate solution. MB dye removal was investigated over pH from 1 to 10 as a function of H^+ concentration shown in Fig. 3. The optimum pH value was observed to be 6 for 55.91% dye removal. In fact, pH is associated with the mechanism of MB adsorption on the PBF adsorbent surface. The chemical formula of methylene blue is $C_{16}H_{18}N_3SCl$, an aromatic compound with a heterocyclic structure. Two mechanisms of adsorption may be planned in such a way (i) chemical reaction between –OH on the PBF surface and Cl^- in MB molecule results in dye removal through eliminating HCl in the system and (ii) electrostatic interaction amid protonated and deprotonated groups at the interface of PBF/MB system (Umoren et al. 2013). At pH $\leq$ 6, the PBF surface is protonated as follows:

$$OH^- + H^+ \rightarrow OH_2^+$$

$$OH_2^+ + D^+ \rightarrow OH_2^+ \dots D^+ (\text{repulsion})$$
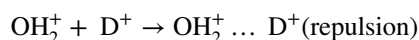
Adsorption decreases at pH $\leq$ 6 due to the cationic interaction of the dye molecule. Nevertheless, optimum pH was considered at pH 6 for MB removal of ~56% point out the fact that at this pH region a combination of Vander Waals Force and the formation of hydrogen bonding are predominant (Umoren et al. 2013). At pH $^>$6, adsorption gradually increased due to deprotonation of the adsorbent and ultimately released free O_2 on the PBF surface. At this condition, the adsorption process ameliorated owing to electrostatic attraction with the cations as presented below:

$$OH^- \rightarrow O^- + H^+$$
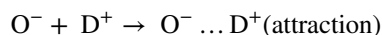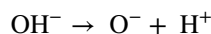
$$O^- + D^+ \rightarrow O^- \dots D^+ (\text{attraction})$$

Therefore, with increasing pH, adsorption for cationic dyes is enhanced as the surface sites of negatively charged on the PBF adsorbent are increased thanks to electrostatic attraction (Senthil Kumar et al. 2010). The adsorption capacity of the as-prepared PBF adsorbent is compared to some other low-cost adsorbents are listed in Table 2.

Effect of adsorbent dosage

The effect of adsorbent dosage on MB uptake by PBF powder is displayed in Fig. 4. The removal efficiency of MB is somehow proportionally affected by various adsorbent dosages. With the increase of PBF adsorbent dosage from 0.25 to 1 g, the dye removal percentage also increased from 29.28 to 59.17%. If the adsorbent dosage is increased again from 1 to 4 g the removal percentage also increases simultaneously from 59.17 to 77.148% and after that the separation percentage becomes constant. The optimum adsorbent dosage of 1 g was obtained for the most favorable efficiency of MB dye removal. Active sites on the PBF adsorbent increased as the more active surface area is available for adsorption due to increasing adsorbent dosage. Banana fiber consists of lignin and cellulose-based plant materials of various active groups as discussed in spectrometric analysis and these functional

Table 2 Comparison of different low-cost adsorbents with removal percentage at operating pH

Adsorbent	Dye	pH	Removal (%)	References
Fly ash	MB	2–8	36–45	Kumar et al. 2005)
Untreated sawdust	Remazol blue	6–10	45–55	Ghosh and Reddy 2013)
Natural coir dust	Remazol Red	2–8	30–40	Ara 2015)
Sugarcane bagasse	MB	5	20–26	Ara 2015)
Banana fiber	MB	1–10	28–56	Present work
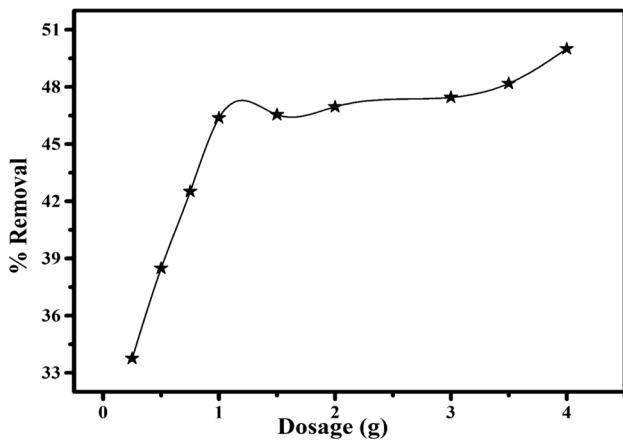
Fig. 4 Impact of PBF adsorbent dosage for MB dye removal from aqueous solution at optimum conditions (pH 6, MB concentration 100 ppm, contact time 12 h)

groups take part in chemical bond formation with dye molecules present in the dye solution. With the increase of PBF adsorbent amount, there is a possibility to increase the separation of MB dye from the solution. The comparison of dye removal percentage of PBF with other low-cost adsorbents is displayed in Table 3.

Effect of initial dye concentration

The initial concentration of MB dye affected the separation efficiency of the adsorption process. The dye percentage of dye separation was decreasing with increasing concentration from 25 to 300 ppm, while the solution pH was fixed to 6, the contact time was maintained for 12 h and adsorbent dosage was constant to 1 g as shown in Fig. 5 because the

adsorbent surface of PBF was saturated with the adsorption sites of MB. At lower concentrations, there are some unused active sites on the adsorbent surface and with increasing initial dye concentration; there will be a shortage of active sites for a fixed amount of adsorbent (Kannan and Sundaram 2001). The driving force required for mass transfer between aqueous (MB) and solid phases (PBF) is increased owing to higher MB concentration point out the possibility of higher molecular collision amid the active groups of the phases (Bulut and Aydın 2006). At low concentration, adsorption sites uptake solute molecules from the MB/PBF system more quickly as well as adsorption takes place at higher energy sites (Horsfall and Spiff 2005). On the contrary, at a higher concentration, the adsorption efficiency decreases as the higher energy sites become saturated and adsorption starts at the sites of lower energy. In this research work, the ideal concentration of the MB dye was found to be 100 ppm with a dye separation efficiency of 57.89%.

The adsorbent activity of PBF at various dye concentrations can be compared with other low-cost adsorbents as displayed in Table 3. It has been found that the separation of methyl orange by chitosan/alumina at different concentrations of 20 to 400 ppm the dye removal percentage decreased from 99.53 to 83.55% (Zhang et al. 2012). Similarly, the separation of MB dye by pine leaves from aqueous solution decreased from 96.5 to 40.9% with the increase of solution concentration from 10 to 90 ppm (Yagub et al. 2012).

Effect of contact time

The contact time effect was investigated by adding 1 g of PBF adsorbent in 100 ml of dye solution with a concentration of 100 ppm at a constant pH of 6 as displayed in Fig. 6. The figure depicts that the increment of contact time from

Table 3 Comparison of the performance of PBF with different low-cost adsorbents regarding various adsorbent dosages

Adsorbent	Dye	Dosage	Removal (%)	References
Pine cone	Congo red	10–30 mg	13.45–18.96	Yagub et al. 2012)
Tea waste	Basic yellow 2	2–20 g	19–60	Afroze et al. 2016)
Cashew nutshells	Congo red	5–30 g	56.3–99.3	Mane and Babu 2011)
Orange peel	Acid violet 17	50–600 mg/50 mL	15–98	Sivaraj et al. 2001)
Rice hull	Reactive orange 16	20–80 mg	21.7–56.2	Ong et al. 2007)
Banana fiber	MB	0.25–4 g	33.75–50	Present work

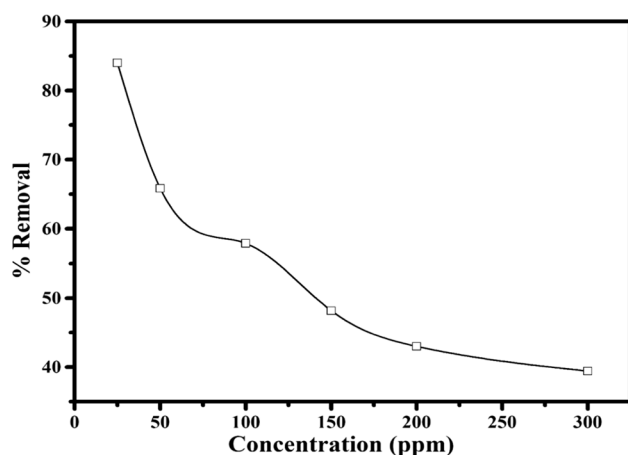**Fig. 5** Impact of initial MB dye concentration on PBF adsorbent at optimum conditions (pH 6, PBF dose 1 g, contact time 12 h)
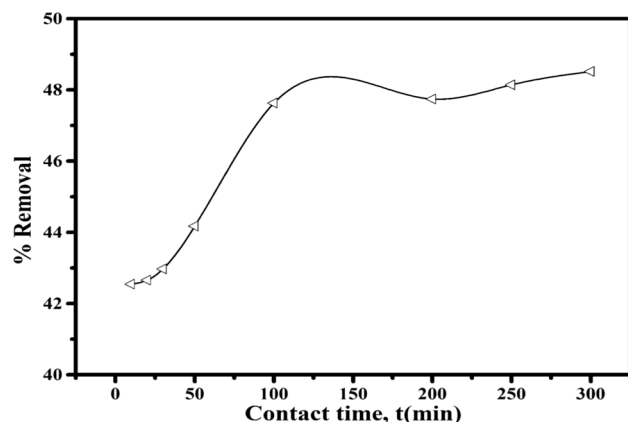
Table 4 Various adsorption isotherm parameters of MB dye adsorbed on PBF

Isotherm	Parameters			R^2
Langmuir	Q_o (mg/g)	K_L (l/mg)	R_L	0.9979
	42.28	2.27	4.386×10^{-3}	
Freundlich	1/n	n	K_f (mg/g)	0.991
	0.30	3.33	0.521	
Temkin	b (l/mg)		k_T	0.9962
	2.7362		0.194	
Dubinin–Rad-hushkevich	q_s (mg/g)	E (kJ/mol)	B (mmol^{2}j^{-2})	0.9296
	7.6875	10.19	4×10^{-5}	

Fig. 6 Impact of contact time for the separation of MB dye on the surface of PBF at optimum conditions (pH 6, PBF dose 1 g, MB concentration 100 ppm)
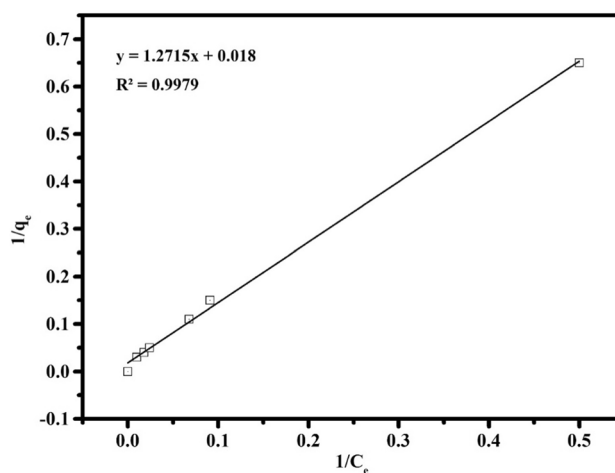
Fig. 7 Langmuir adsorption isotherm for the adsorption of MB dye on PBF surface

10 to 300 min improves the MB dye separation percentage. Initially, the dye uptake activity was slower for 10 min. The variety of adsorbents and their reactive functional groups affect the adsorption kinetics of the system. The optimum for the adsorption of MB dye on the PBF adsorbent was found to be 100 min with a dye uptake capacity of around 47.63%. To consider the adsorption process of the clarified sludge/rice husk system, a contact time of 2 h was required to establish equilibrium. In the case of some other adsorbents, the physical properties of adsorption were conducted for a contact time of 2–5 h to confirm equilibrium conditions (Macedo et al. 2008).

Adsorption isotherms

Adsorption isotherm is a vital parameter to analyze the adsorption data that helps to understand the adsorption mechanism of MB molecule on the PBF. Four adsorption isotherms of Langmuir, Freundlich, Temkin, and Dubinin–Radushkeyich models were used to fit the adsorption data of the MB/PBF system. Additionally, Table 4 describes the adsorption parameters obtained from the fittings of the isotherm models.

Langmuir adsorption isotherm

Langmuir isotherm indicates the monolayer adsorption mechanism of MB dye on the surface of the PBF. According to this isotherm model, only one layer of adsorption takes place and after the first layer of adsorption, no adsorbate is adsorbed on the adsorbent surface. The plot of $1/q_e$ versus $1/C_e$ results in a linear line shown in Fig. 7 and the extracted values of the parameters are inserted in Table 4. The highest monolayer coverage (Q_0) was computed from the intercept and slope of the linear fitting, respectively (Chakraborty et al. 2011). The adsorption capacity of the PBF (Q_o) from the isotherm model was calculated as 42.28 mg/g, K_L 2.27 l/

mg and R_L 4.386×10^{-3} results in favorable conditions for equilibrium sorption (Table 4). The value of R^2 is 0.9979 which is very close to one indicating the better fitting of the isotherm model. According to this model, the MB adsorbate molecules are homogeneously distributed over the surface of the PBF and monolayer adsorption has been assumed. According to Fig. 7, the value of the separation factor, $R_L \cdot 0$ but $R_L \cdot 1$ designates that the adsorption isotherm is promising. In a nut shell, the Langmuir adsorption isotherm is the best fitted model (R^2) as regards the data extracted from the fittings of the additional isotherm models.

Freundlich adsorption isotherm

According to the Freundlich isotherm model, both physisorption and chemisorption take place. In this model, first monolayer adsorption takes place and after that multilayer adsorption occurs through physisorption. The isotherm model is presented in Fig. 8 and the adsorption data are displayed in Table 4. The values of $1/n$, n, K_f, and R^2 were found to be 0.30, 3.33, 0.521 mg/g and 0.991, respectively. Freundlich adsorption constant n describes the adsorption mechanism and $1/n$ is the function of the adsorption strength. If the value of n is higher than one ($n > 1$), the adsorption is favorable and if the value is less than one ($n < 1$), the process is unfavorable (Chakraborty et al. 2011). Moreover, K_f is the adsorption constant which implies the indicator of adsorption capacity (Bentahar et al. 2016). Therefore, according to this model, heterogeneous adsorption is suspected.

Temkin adsorption isotherm

By plotting q_e versus $\ln C_e$, a linear line was obtained as displayed in Fig. 9. K_T and B are the isotherm constants
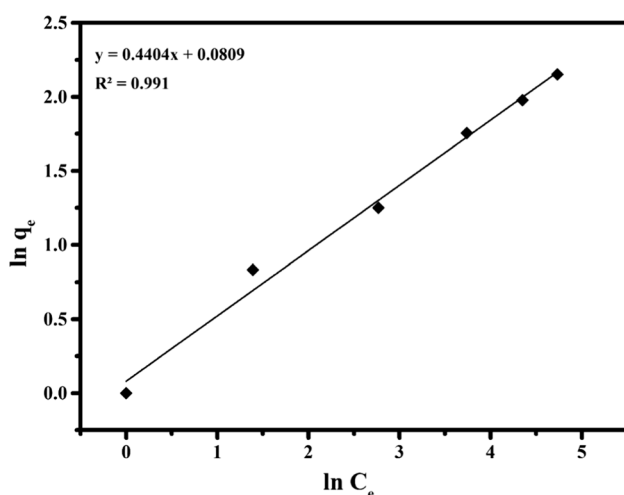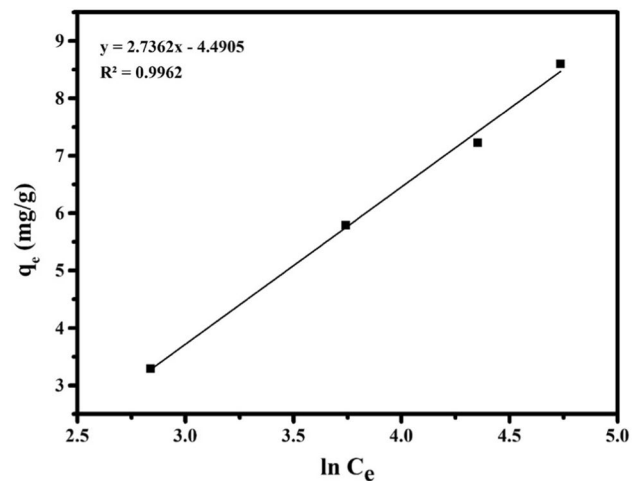

Fig. 9 Temkin adsorption isotherm of MB dye adsorption on the PBF surface

which were computed from the slope and intercept of the line. Here, K_T is related to the binding energy and B corresponds to the heat of adsorption. It was found that the heat of adsorption is decreased during layer formation by the MB molecules on the surface of the PBF adsorbent due to the interaction between adsorbate and adsorbent substances (Bhattacharya et al. 2008a). The values of the isotherm constants (K_T and B) and correlation factor (R^2) are displayed in Table 4.

Dubinin–Radushkevich adsorption isotherm

Dubinin–Radushkeyich isotherm is also an important model for the fitting of adsorption data. In this isotherm model, a straight line was found by plotting $\ln q_e$ versus ε^2 (Fig. 10); the isotherm constants q_s and E were then measured from the intercept and slope of the line, accordingly. The estimated values of the adsorption parameters are displayed in Table 4. Here, the q_s cx represents the adsorption capacity, and the adsorption saturation point for MB on the banana fiber adsorbent was determined by this adsorption isotherm model. The value of E indicates the types of adsorption taking place, for instance, if the value is 8–16 kJ/mol chemical adsorption will occur; similarly, if the value is less than 8 kJ/mol physical adsorption will take place (Chowdhury and Saha 2010). In the current issue the value was found to be 10.19 kJ/mol results in indicating MB chemically adsorbed on the surface of the low-cost adsorbent.

Adsorption kinetics

The kinetic property of a liquid/solid adsorption system is an essential parameter to measure the rate of adsorption. Lagergren pseudo-first-order and second-order models
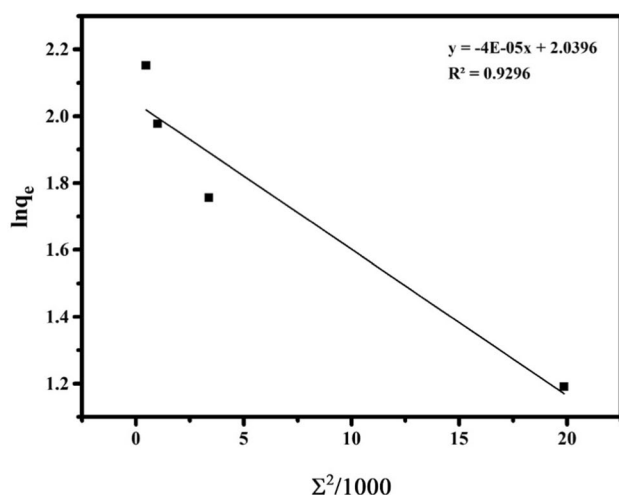

Fig. 8 Freundlich adsorption isotherm of MB dye adsorption on the PBF surface

Fig. 10 Dubinin–Radhushkevich adsorption isotherm of MB dye adsorption on the PBF surface

Fig. 11 Pseudo-first-order kinetic model for the adsorption of MB dye on the PBF surface

based on the adsorption kinetic data were evaluated at different initial concentrations. According to the first-order model, the adsorption rate is proportional to the first power of the concentration. The sorption capacity of the solid phase can be determined by the pseudo-second-order model. Similarly, this model reveals that chemisorption takes place between adsorbate and adsorbent which is the rate-determining step of this kind.

Lagergren pseudo-first-order

According to Fig. 11, a linear line was found by plotting $log(q_e - q_t)$ versus t for the first-order kinetics, which helps to determine the rate constant k_1 from the slope of the linear fitting. The linearity of the plot results in the mechanism of the first-order adsorption. The rate constant k_1 value of the model was determined to be 8.7×10^3 (min^{-1}) from the least square method for the MB/PBF system along with the correlation coefficient of $R^2 = 0.9964$.

Pseudo-second-order

The plot of t/q_e versus t of the pseudo-second-order kinetic equation demonstrates somehow a linear relationship point out the values of k_2 and q_e corresponding to the intercept and slope (Fig. 12). Rate constant k_2 and the value of correlation coefficient (R^2) were found to be 5.03×10^2 and 0.999, respectively. The values of R^2 revealed the better fitting of the kinetic data compared to the first-order model to uptake MB from dye enriched water.
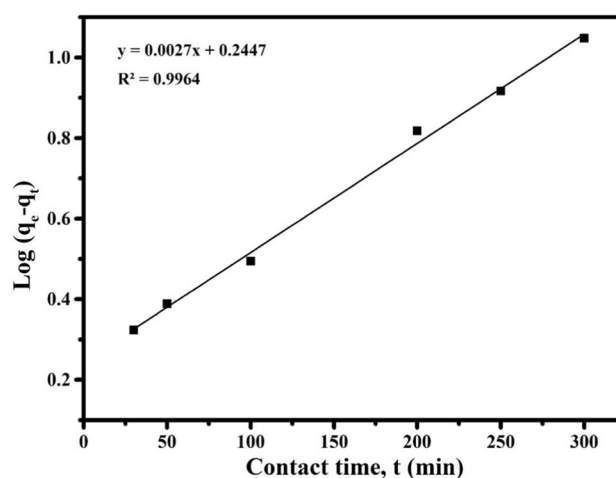
Mass transfer analysis

The mass transfer model of the MB/PBF system can be explained by the plot of $ln[C_t/C_o - 1/(1 + MK_{bq})]$ versus t showed a linear line (Fig. 13). Mass transfer coefficient β was graphically evaluated from the slope $[(1 + MK_{bq}/MK_{bq})\beta S_s]$ of the plot and the value was found to be 1.45×10^3 ($R^2 = 0.9962$) which point out that transporting velocity of MB dye from the bulk solution to the solid PBF surface is very fast. Similar phenomenon also reported elsewhere (Coconut tree bark as a potential low-cost adsorbent for the removal of methylene blue from wastewater 2019; Bhattacharya et al. 2008b).
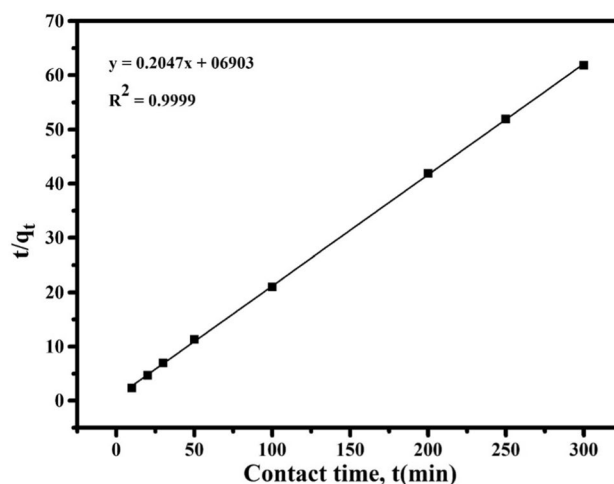

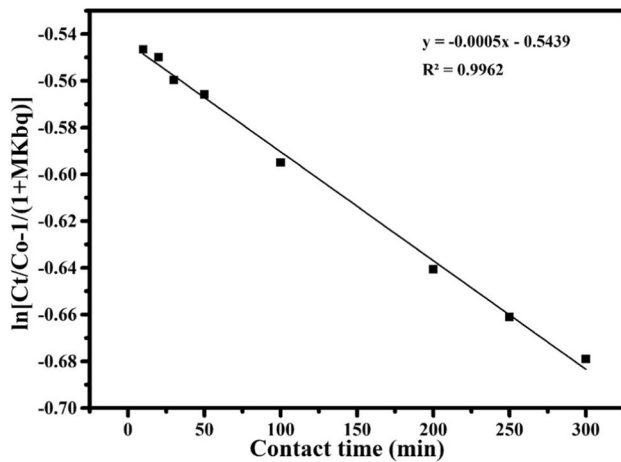**Fig. 12** Pseudo-second-order kinetic model for the adsorption of MB dye on the PBF surface

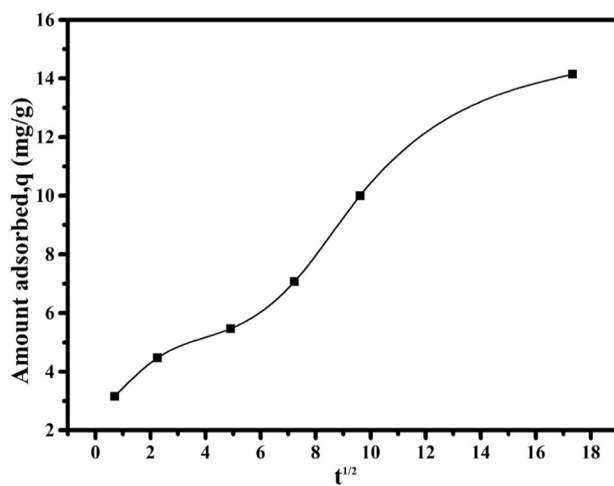**Fig. 13** Mass transfer plot for the MB dye adsorption on the PBF surface

Fig. 14 Weber and Morris diffusion model for the separation of MB dye on PBF adsorbent surface

Weber and Morris intra-particle diffusion

Steps involved in the adsorption of MB by means of PBF powder include transportation of dye molecules from the bulk phase to the solid surface followed by diffusion of the solute molecules into the pores. This diffusion is generally known as a slow rate-determining process. The adsorption process for the MB/PBF system at a certain pH 6 and PBF dosage of 1.0 g did not show a linear relationship over the time period representing that more than one phenomenon are involved during the adsorption (Fig. 14). The intra-particle diffusion coefficient was determined from the slope of the plot q versus $t^{1/2}$ and the value was obtained to be $K_{id} = 0.42$ mg g^{-1} min$^{-1/2}$. After a certain time of diffusion, almost a linear relationship was observed from the figure but

the curve did not go through the origin. The reason behind such characteristics is the boundary layer effect that draws attention toward the mechanism of MB adsorption on the PBF surface to be complex and intra-particle diffusion is also a contributor at the time of the rate-determining step. The surface sorption largely depends on the intercept and with the increase of the intercept, the surface sorption also increased. The intercept and diffusion coefficient values of the plot increase with an increase in the initial MB dye concentrations. In fact, the initial portion of the diffusion curve is attributed to mass transfer and the linear portion is related to intra-particle diffusion (Nipa et al. 2019). Parvin et al. studied intra-particle diffusion model for the MB dye adsorption by coconut tree bark, which points out that the adsorption process has boundary layer effect (Parvin et al. 2019).

Adsorption mechanism

It is very important to figure out the mechanism of the adsorption to remove MB dye from the aqueous solution to the adsorbent surface. The adsorption process can be described based on the chemistry of the PBF adsorbent surface. FTIR is a useful technique to observe the interaction among adsorbate molecules and active sites existing on the surface of the adsorbent (Ahmad et al. 2012). PBF is polysaccharides by nature containing lignin, cellulose, and hemicellulose with polyphenolic groups. The surface functional groups are possibly useful for bond formation with reactive adsorbate molecules over different mechanisms. Besides, FTIR of the PBF adsorbent revealed the reactive groups of C=O and OH are in abundance. The PBF adsorbent is made out of different materials like lignin, cellulose, and β cellulose with some minor compounds (oil, protein, starch, etc.) (Senthil Kumar et al. 2010). Oxygen-containing functional groups (C=O, –C–O–C– and OH) are existed in large in β cellulose and cellulose. However, lignin having polymerized structure is a complex compound, which contains an aromatic substance and functions as a cementing matrix. These binding elements then hold mutual contributions of β cellulose and cellulose units (Bulut and Aydın 2006). Different properties of the adsorbent like functional groups, pH, and size of the pore play vital roles in understanding the sorption mechanism. The as-produced PBF is acidic in nature (pH 5.61) owing to the functional groups of alcohols, phenolic hydroxide, ethers, carboxylic acid, etc. The chemisorption occurs through hydrogen bonding among OH groups of PBF surface and Cl$^-$/N atoms of the MB dye. The MB adsorption on the PBF adsorbent surface might take place either by charge localization or by aromatic rings containing in the basic dye. These aromatic rings are oriented in horizontal or perpendicular to the surface. The adsorption by charge localization is occurred by the hydrogen bonding between

the active site of the adsorbent surface and one of the –NH$_2$ groups present in the dye molecules. The orientation of the aromatic rings in the dye molecules is possibly oriented in the horizontal axis and this type of bonding is formed by either electrostatic force or by hydrogen bonding through the resonance structure of the MB dye (Bulut and Aydın 2006). However, the key mechanism of the adsorption is the charged surface and electrostatic attraction amid the dye molecules. The expected mechanism for the adsorption of MB dye on PBH is displayed in Fig. 15. A similar adsorption mechanism has been reported by Rahman et. al (Alencar et al. 2012) where date palm fiber was used as an adsorbent to remove heavy metal (chromium-VI) from industrial wastewater.

Discussion

In this investigation, we optimized pH 6, MB concentration 100 ppm, PBF adsorbent dosages 1 g, and PBF/MB contact time for 100 min. The maximum dye removal percentage was found at pH 6. Dye concentration also manipulated the adsorption process and dye removal decreased with increasing the MB dye concentration. The initial concentration has been optimized at 100 ppm. Adsorbent doses are directly proportional to the dye removal and the optimum adsorbent dosage is 1 g. A kinetic study of the adsorption process was performed based on interaction time. In fact, with increasing interaction time, the dye removal efficiency rises and the optimized value of the time was obtained 100 min. The data

Table 5 Comparison of different low-cost adsorbents based on MB dye adsorption capacity of PBF

Adsorbent	Adsorption capacity (mg/g)	References
Orange peel	14.3	Annadural et al. 2003)
Sugarcane dust	3.8	Khattri and Singh 1999)
Neem sawdust	3.8	Khattri and Singh 2009)
Sugarcane fiber	10.44	Parab et al. 2009)
Jalshakti® polymer	12.9	Dhodapkar et al. 2007)
Banana fiber	42.28	Present study

well fitted with the pseudo-second-order kinetics model. The effect of the equilibrium concentration of MB removal was simulated by fitting the adsorption data in different adsorption isotherms. Table 5 represents the comparable adsorption performance of numerous low-cost adsorbents to remove dyes from industrial wastewater. It can be observed from the table that PBF adsorbent has a superior adsorption ability of 42.28 mg/g than the others extracted from the literature reviews. Therefore, banana fiber can be recognized as a potential low-cost adsorbent for the separation of organic dyes from wastewater.

In addition, regeneration of the used adsorbent and adsorbate is massive important to make the process economically viable. In this context, at a higher acidic and basic environment, the electrostatic attraction between the dye and adsorbent is significantly lower; hence simple washing by highly acidic or basic pH solution could give recovery of
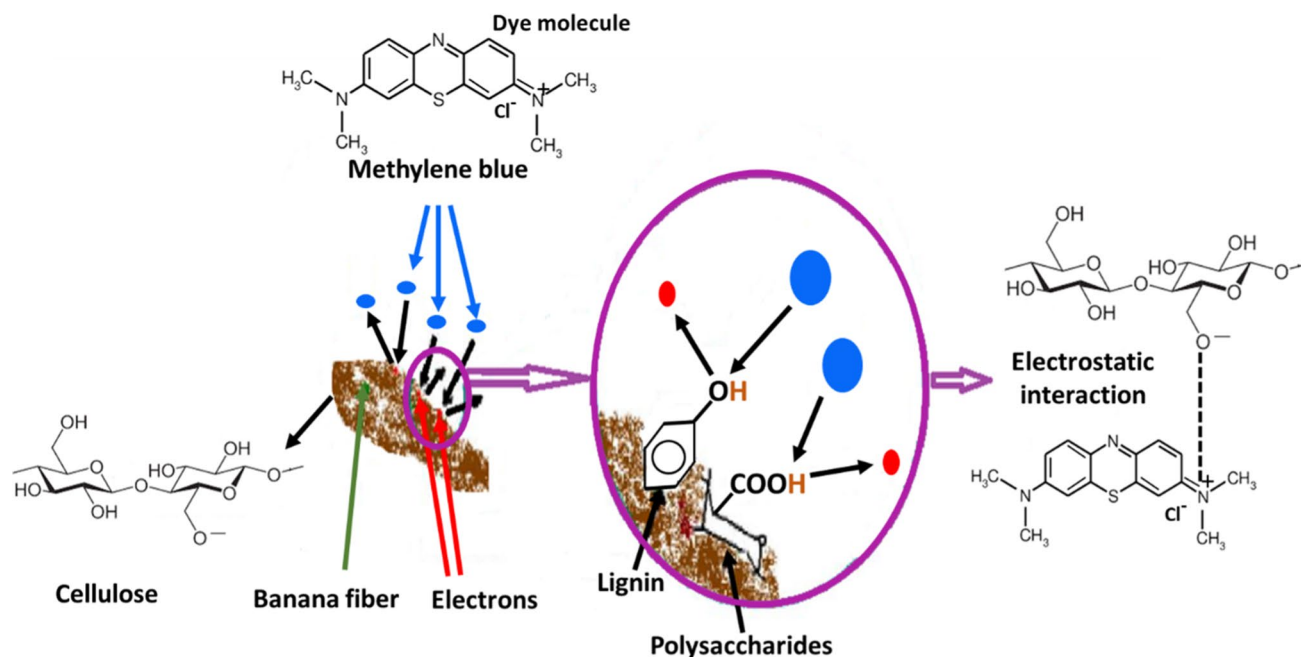

Fig. 15 Plausible adsorption mechanism for the separation of MB dye on the PBF surface

the PBF adsorbent and the MB dye. Besides, chemical treatment or other regeneration methods (Momina and Isamil 2018) would be employed. In fact, regeneration method is very important for economic and environmental aspects. Nowadays, the new generation is rapidly switching toward bio-based clean energy resources (Alam et al. 2014) as well as piezoelectric power generation (Shawon et al. 2022) to overcome global energy crisis.

Conclusion

Banana fiber has been demonstrated in the current issue as a suitable adsorbent for the elimination of dyes from industrial wastewater. Different adsorption properties like initial concentration, pH, contact time, and adsorbent dosages of PBF/MB were optimized for the highest separation of the dye. The higher the concentration of the dye results in the lower percentage of the MB uptake from the aqueous solution, whereas, dye separation percentage can be enhanced by increasing the adsorption contact time and increasing the addition of adsorbent dosage. Moreover, adsorbent dosage in higher quantity ameliorates MB adsorption because of the greater number of active sites present in the system. A kinetic study of the adsorption process was conducted and it has been observed that the adsorption process followed the pseudo-second-order kinetics model. The equilibrium data of the dye removal was tailored by the adsorption isotherms of Langmuir, Freundlich, Temkin, and Dubinin–Radushkevich. The obtained results indicate that adsorption of MB dye on the surface of PBF involved the complex mechanism of adsorption and two distinct stages. The other two adsorption stages comprised of the diffusion of the dye molecules through the boundary layer because of the external mass transfer effect and the intra-particle diffusion which helps during rate-determining steps.

Declarations

Conflict of interest The authors declare that they have no known competing financial interest or personal relationships that could have appeared to influence the work reported in this paper.

Ethical approval The authors declare that this paper complies with generally accepted ethical standards. The authors confirm that they followed the rules of ethics in preparing the article and conducting the research.

References

Abraham E, Deepa B, Pothan LA, Jacob M, Thomas S, Cvelbar U, Anandjiwala R (2011) Extraction of nanocellulose fibrils from lingo cellulosic fibres: a novel approach. Carbohyd Polym 86(4):1468–1475. https://doi.org/10.1016/j.carbpol.2011.06.034

Adebayo MA, Prola LDT, Lima EC, Puchana–rosero MJ, Saucier C, Umpierres, CS, Vaghetti JCP, Catalu R, Leandro G, Ruggiero R (2014) Adsorption of procion blue MX–R dye from aqueous solutions by lignin chemically modified with aluminium and manganese. 268, 43–50. https://doi.org/10.1016/j.jhazmat.2014.01.005

Afroze S, Sen TK, Ang M, Nishioka H (2016) Adsorption of methylene blue dye from aqueous solution by novel biomass *Eucalyptus sheathiana* bark: equilibrium, kinetics, thermodynamics and mechanism. Desalin Water Treat 57(13):5858–5878. https://doi.org/10.1080/19443994.2015.1004115

Ahmad T, Danish M, Rafatullah M, Ghazali A, Sulaiman O, Hashim R, Ibrahim MNM (2012) The use of date palm as a potential adsorbent for wastewater treatment: a review. Environ Sci Pollut Res 19(5):1464–1484. https://doi.org/10.1007/s11356-011-0709-8

Alam MJ, Shawon SM, Sultana M, Rahman MW, Khan MM (2014) Kinetic study of biodiesel production from soybean oil. In: 2014 power and energy systems: towards sustainable energy, pp 1–5

Alam J, Das BC, Rahman W, Kumar B, Khan MR (2015) Removal of dark blue-GL from wastewater using water hyacinth : a study of equilibrium adsorption isotherm. Desalin Water Treat 56(6):1520–1525. https://doi.org/10.1080/19443994.2014.950996

Alencar WS, Acayanka E, Lima EC, Royer B, de Souza FE, Lameira J, Alves CN (2012) Application of *Mangifera indica* (mango) seeds as a biosorbent for removal of Victazol Orange 3R dye from aqueous solution and study of the biosorption mechanism. Chem Eng J 209:577–588. https://doi.org/10.1016/j.cej.2012.08.053

Álhusseiny HA (2014) Adsorption of methylene blue dye using low cost adsorbent of sawdust: batch and continues studies. J Babylon Univ Eng Sci 22(2):296–310

Ali MY, Rahman MW, Moniruzzaman M, Alam MJ, Saha I, Halim MA, Deb A, Sumi MSA, Parvin S, Biswas10, BK(2016). *Nypa fruticans* as a potential low cost adsorbent to uptake heavy metals from industrial wastewater. In: Full Paper Proceeding ECBA, 55(5):18–25. http://umpir.ump.edu.my/id/eprint/13433/

Almeida EJR, Corso CR (2014) Chemosphere comparative study of toxicity of azo dye procion red MX–5B following biosorption and biodegradation treatments with the fungi *Aspergillus niger* and *Aspergillus terreus*. Chemosphere 112:317–322. https://doi.org/10.1016/j.chemosphere.2014.04.060

Amel K, Hassen MA, Kerroum D (2012) Isotherm and kinetics study of biosorption of cationic dye onto banana peel. Energy Procedia 19:286–295. https://doi.org/10.1016/j.egypro.2012.05.208

Ángel J, López S, Li Q, Thompson IP, Ángel J, López S, Li Q, Thompson IP (2010) Biorefinery of waste orange peel. Crit Rev Biotechnol 30(1):63–69. https://doi.org/10.3109/07388550903425201

Annadural G, Juang RS, Lee DJ (2003) Adsorption of heavy metals from water using banana and orange peels. Water Sci Technol 47(1):185–190 (**PMID: 12578193**)

Ara NJ (2015) Development of dyes removal method from textile waste water development of dyes removal method from textile waste water doctor of philosophy in chemistry. http://repository.library.du.ac.bd/xmlui/bitstream/handle/123456789/1112/Nargish%20Jahan.pdf?sequence=1&isAllowed=y

Bentahar Y, Hurel C, Draoui K, Khairoun S, Marmier N (2016) Adsorptive properties of Moroccan clays for the removal of arsenic(V) from aqueous solution. Appl Clay Sci 119:385–392. https://doi.org/10.1016/j.clay.2015.11.008

Bessegato GG, Cardoso JC, Valnice M, Zanoni B (2014) Enhanced photoelectrocatalytic degradation of an acid dye with boron–doped TiO_2 nanotube anodes. Catal Today. https://doi.org/10.1016/j.cattod.2014.03.073

Bhattacharya AK, Naiya TK, Mandal SN, Das SK (2008a) Adsorption, kinetics and equilibrium studies on removal of Cr(VI) from aqueous solutions using different low-cost adsorbents. Chem Eng J 137(3):529–541. https://doi.org/10.1016/j.cej.2007.05.021

Bhattacharya AK, Naiya TK, Mandal SN, Das SK (2008b) Adsorption, kinetics and equilibrium studies on removal of Cr (VI) from aqueous solutions using different low-cost adsorbents. Chem Eng J 137:529–541

Bilba K, Arsene MA, Ouensanga A (2007) Study of banana and coconut fibers. Botanical composition, thermal degradation and textural observations. Bioresour Technol 98(1):58–68

Bulut Y, Aydın H (2006) A kinetics and thermodynamics study of methylene blue adsorption on wheat shells. Desalination 194(1):259–267. https://doi.org/10.1016/j.desal.2005.10.032

Calvert JG (1990) Glossary of atmospheric chemistry terms. Pure Appl Chem 62(11):2167–2219. https://doi.org/10.1351/pac199062112167

Chakraborty S, Chowdhury S, Das Saha P (2011) Adsorption of crystal Violet from aqueous solution onto NaOH-modified rice husk. Carbohyd Polym 86(4):1533–1541. https://doi.org/10.1016/j.carbpol.2011.06.058

Chen W, Feng J, Renguang W (2013) Roles of ENSO and PDO in the link of the East Asian winter monsoon to the following summer monsoon. J Clim 26(2):622–635. https://doi.org/10.1175/JCLI-D-12-00021.1

Chowdhury S, Saha P (2010) Sea shell powder as a new adsorbent to remove Basic Green 4 (Malachite Green) from aqueous solutions: Equilibrium, kinetic and thermodynamic studies. Chem Eng J 164(1):168–177. https://doi.org/10.1016/j.cej.2010.08.050

Demirbas E, Kobya M, Senturk E, Ozkan T (2004) Adsorption kinetics for the removal of chromium (VI) from aqueous solutions on the activated carbons prepared from agricultural wastes. Water SA 30(4):533–539

Dhodapkar R, Rao NN, Pande SP, Nandy T, Devotta S (2007) Adsorption of cationic dyes on Jalshakti®, super absorbent polymer and photocatalytic regeneration of the adsorbent. React Funct Polym 67(6):540–548. https://doi.org/10.1016/j.reactfunctpolym.2007.03.007

Doumic L, Salierno G, Cassanello M, Haure P, Ayude M (2014) supported over alumina. Catal Today. https://doi.org/10.1016/j.cattod.2014.03.064

El-Sayed GO (2011) Removal of methylene blue and crystal violet from aqueous solutions by palm kernel fiber. Desalination 272(1–3):225–232. https://doi.org/10.1016/j.desal.2011.01.025

Emilia M, Vanesa G, Ricardo P, Lea A (2014) Activated carbon developed from orange peels : batch and dynamic competitive adsorption of basic dyes. Ind Crops Prod 62:437–445. https://doi.org/10.1016/j.indcrop.2014.09.015

Faur-brasquet C, Le Cloirec P (2003) Adsorption of dyes onto activated carbon cloths : approach of adsorption mechanisms and coupling of ACC with ultrafiltration to treat coloured wastewaters. 31 3–11

Garg VK, Amita M, Kumar R, Gupta R (2004) Basic dye (methylene blue) removal from simulated wastewater by adsorption using Indian rosewood sawdust: a timber industry waste. https://doi.org/10.1016/j.dyepig.2004.03.005

Ghosh RK, Reddy DD (2013) Tobacco stem ash as an adsorbent for removal of methylene blue from aqueous solution: equilibrium, kinetics, and mechanism of adsorption. Water Air Soil Pollut. https://doi.org/10.1007/s11270-013-1582-5

Gouamid M, Ouahrani MR, Bensaci MB (2013) Adsorption equilibrium, kinetics and thermodynamics of methylene blue from aqueous solutions using date palm Leaves. Energy Procedia 36:898–907. https://doi.org/10.1016/j.egypro.2013.07.103

Guechi EK, Hamdaoui O (2016) Biosorption of methylene blue from aqueous solution by potato (Solanum tuberosum) peel: equilibrium modelling, kinetic, and thermodynamic studies. Desalin Water Treat 57(22):10270–10285. https://doi.org/10.1080/19443994.2015.1035338

Harvey JW, Keitt AS (1983) Studies of the efficacy and potential hazards of methylene blue therapy in aniline-induced methaemoglobinaemia. Br J Haematol 54(1):29–41. https://doi.org/10.1111/j.1365-2141.1983.tb02064.x

Helmer R, Hespanhol I, Nations U, Programme E, Council SC (n.d.) (1998) Water pollution control—a guide to the use of water quality management principles. London: E & FN Spon. https://apps.who.int/iris/handle/10665/41967

Hemsas S, Lounici H, And ZB, Benrachedi K (2014) Removal of dispersed dyes from aqueous solution using activated carbon prepared from olive stones. J Agric Sci Technol A 4. https://www.researchgate.net/publication/265086434

Ho YS, McKay G, Wase DAJ, Forster CF (2000) Study of the sorption of divalent metal ions on to peat. Adsorpt Sci Technol 18(7):639–650. https://doi.org/10.1260/0263617001493693

Horsfall M, Spiff AI (2005) Kinetic studies on the sorption of lead and cadmium ions from aqueous solutions by Caladium bicolor (wild cocoyam) biomass. In Bulletin of the chemical society of ethiopia (Vol. 19, Issue 1, pp. 89–102). https://doi.org/10.4314/bcse.v19i1.21114

Ibrahim M (2002) Preparation of cellulose and cellulose derivative azo compounds. Cellulose 9(3–4):337–349. https://doi.org/10.1023/A:1021154204053

Ibrahim MM, Dufresne A, El-Zawawy WK, Agblevor FA (2010) Banana fibers and microfibrils as lignocellulosic reinforcements in polymer composites. Carbohydr Polym 81(4):811–819. https://doi.org/10.1016/j.carbpol.2010.03.057

Indhumathi PSSSP Saraswathy CP (2011) The identification and characterization of activated carbon for adsorption studies. Int J Adv Eng Technol 2(3):78–84

Jawad AH, Rashid RA, Mahmuod RMA, Ishak MAM, Kasim NN, Ismail K (2016) Adsorption of methylene blue onto coconut (Cocos nucifera) leaf: optimization, isotherm and kinetic studies. Desalin Water Treat 57(19):8839–8853. https://doi.org/10.1080/19443994.2015.1026282

Kannan N, Sundaram MM (2001) Kinetics and mechanism of removal of methylene blue by adsorption on various carbons—a comparative study. Dye Pigm 51(1):25–40. https://doi.org/10.1016/S0143-7208(01)00056-0

Khan TA, Rahman R, Ali I, Khan EA, Mukhlif AA (2014) Removal of malachite green from aqueous solution using waste pea shells as low–cost adsorbent—adsorption isotherms and dynamics. Toxicol Environ Chem 96(4):569–578. https://doi.org/10.1080/02772248.2014.969268

Khan MM, Rahman MW, Ong HR, Ismail AB, Cheng CK (2016) Tea dust as a potential low−cost adsorbent for the removal of crystal violet from aqueous solution. Desalin Water Treat 57(31):14728–14738

Khattri SD, Singh MK (1999) Colour removal from dye wastewater using sugar cane dust as an adsorbent. Adsorpt Sci Technol 17(4):269–282. https://doi.org/10.1177/026361749901700404

Khattri SD, Singh MK (2009) Removal of malachite green from dye wastewater using neem sawdust by adsorption. J Hazard Mater 167(1–3):1089–1094. https://doi.org/10.1016/j.jhazmat.2009.01.101

Kumar KV, Ramamurthi V, Sivanesan S (2005) Modeling the mechanism involved during the sorption of methylene blue onto fly ash. J Colloid Interface Sci 284(1):14–21. https://doi.org/10.1016/j.jcis.2004.09.063

Lehr, Jay H., Tyler E. Gass, and W. Pettyjohn (1980) Domestic water treatment." McGraw Hill Book Co. New York 33093 : 272.

Lüttge U, Kluge M, Bauer G (1992) Botanique–Traité Fondamental. Tec & Doc Lavoisier, France

Macedo JS, Otubo L, Ferreira OP, de Gimenez IF, Mazali IO, Barreto LS (2008) Biomorphic activated porous carbons with complex microstructures from lignocellulosic residues. Microporous Mesoporous Mater 107(3):276–285. https://doi.org/10.1016/j.micromeso.2007.03.020

Mane VS, Babu PVV (2011) Studies on the adsorption of Brilliant Green dye from aqueous solution onto low-cost NaOH treated sawdust. Desalination 273(2–3):321–329. https://doi.org/10.1016/j.desal.2011.01.049

McKay G, Otterburn MS, Sweeney AG (1981) Surface mass transfer processes during colour removal from effluent using silica. Water Res 15(3):327–331. https://doi.org/10.1016/0043-1354(81)90036-1

Md. Ferdus Alam (2021) Properties, manufacturing process and application of Banana fiber. https://textilelearner.blogspot.com/2014/01/properties-of-banana-fiber.html

Mokhlesi B, Leikin JB, Murray P (2003) Critical care review adult toxicology in critical care * part II : specific poisonings. Chest 123(3):897–922. https://doi.org/10.1378/chest.123.3.897

Muthuraman G (2011) Extractive removal of astacryl blue BG and astacryl golden yellow dyes from aqueous solutions by liquid–liquid extraction. DES 277(1–3):308–312. https://doi.org/10.1016/j.desal.2011.04.047

Nipa ST, Rahman MW, Saha R, Hasan MM, Deb A (2019) Jute stick powder as a potential low-cost adsorbent to uptake methylene blue from dye enriched wastewater. Desalin Water Treat 153:279–287

Okoronkwo AE, Anwasi S (2008) Biosorption modeling of copper and zinc adsorption from aqueous Solution by tithonia diversifolia. In: CSN conference proceeding. chemical society of Nigeria. Deltachem, pp 92−102. https://www.researchgate.net/publication/285713102

Ong ST, Lee CK, Zainal Z (2007) Removal of basic and reactive dyes using ethylenediamine modified rice hull. Biores Technol 98(15):2792–2799. https://doi.org/10.1016/j.biortech.2006.05.011

Ozmen EY, Sezgin M, Yilmaz A, Yilmaz M (2008) Synthesis of β-cyclodextrin and starch based polymers for sorption of azo dyes from aqueous solutions. 99:526–531. https://doi.org/10.1016/j.biortech.2007.01.023

Parab H, Sudersanan M, Shenoy N, Pathare T, Vaze B (2009) Use of agro-industrial wastes for removal of basic dyes from aqueous solutions. Clean: Soil, Air, Water 37(12):963–969

Parvin S, Rahman MW, Saha I, Alam MJ, Khan MM (2019) Coconut tree bark as a potential low-cost adsorbent for the removal of methylene blue from wastewater. Desalin Water Treat 146:385–392

Prola LDT, Acayanka E, Lima EC, Umpierres CS, Vaghetti JCP, Oliveira W, Laminsi S, Djifon PT (2013) Comparison of Jatropha curcas shells in natural form and treated by non-thermal plasma as biosorbents for removal of reactive red 120 textile dye from aqueous solution. Ind Crops Prod 46:328–340. https://doi.org/10.1016/j.indcrop.2013.02.018

Robinson T, Mcmullan G, Marchant R, Nigam P (2001) Remediation of dyes in textile effluent: a critical review on current treatment technologies with a proposed alternative. 77:247–255. https://doi.org/10.1016/s0960-8524(00)00080-8

Rotliwala YC, Chevli MH, Maheshwari N (n.d.) (2015) Isotherm studies of equilibrium sorption of Fe (III) Onto Unmodified Hen Eggshell Adsorbent. iii, 1–8. https://fdocuments.net/document/isotherm-studies-of-equilibrium-sorption-issue14pdf-isotherm-studies-of-equilibrium.html

Seader Junior D, Ernest J Henley (2011) Separation process principles. https://imtk.ui.ac.id/wp-content/uploads/2014/02/Separation-Process-Principles-Third-Edition.pdf

Senthil Kumar P, Ramalingam S, Senthamarai C, Niranjanaa M, Vijayalakshmi P, Sivanesan S (2010) Adsorption of dye from aqueous solution by cashew nut shell: studies on equilibrium isotherm, kinetics and thermodynamics of interactions. Desalination 261(1–2):52–60. https://doi.org/10.1016/j.desal.2010.05.032

Shahadat M, Isamil S (2018) Regeneration performance of clay–based adsorbents for the removal of industrial dyes: a review. RSC Adv 8(43):24571–24587. https://doi.org/10.1039/c8ra04290j

Shakoor S, Nasar A (2016) Removal of methylene blue dye from artificially contaminated water using citrus limetta peel waste as a very low cost adsorbent. J Taiwan Inst Chem Eng 66:154–163. https://doi.org/10.1016/j.jtice.2016.06.009

Shawon SMAZ, Carballo ZD, Vega VS, Lin C, Rafaqut MS, Sun AX, James Li J, Uddin MJ (2022) Surface modified hybrid ZnSnO3 nanocubes for enhanced piezoelectric power generation and wireless sensory application. Nano Energy 92:106653. https://doi.org/10.1016/j.nanoen.2021.106653

Sivaraj R, Namasivayam C, Kadirvelu K (2001) Orange peel as an adsorbent in the removal of acid violet 17 (acid dye) from aqueous solutions. Waste Manag 21(1):105–110. https://doi.org/10.1016/S0956-053X(00)00076-3

Taylor P, Mahmoodi NM, Khorramfar S (2013) Degradation of dyes using combined photo-Fenton/activated carbon: synergistic effect. Desalin Water Treat. https://doi.org/10.1080/19443994.2013.810378

Taylor P, Gupte S, Keharia H, Gupte A (2015.) Desalination and water treatment toxicity analysis of azo red BS and methyl red dye solutions on earthworm (Pheretima phosthuma), micro-organisms, and plants. pp 37–41. https://doi.org/10.1080/19443994.2012.748637

Umoren SA, Etim UJ, Israel AU (2013) Adsorption of methylene blue from industrial effluent using poly (vinyl alcohol). J Mater Environ Sci 4(1):75–86

Vučurović VM, Razmovski RN, Miljić UD, Puškaš VS (2014) Removal of cationic and anionic azo dyes from aqueous solutions by adsorption on maize stem tissue. J Taiwan Inst Chem Eng 45(4):1700–1708. https://doi.org/10.1016/j.jtice.2013.12.020

Weber WJ, Morris JC (1963) Kinetics of adsorption on carbon from solution. J Sanit Eng Div 89(2):31–60

Yagub MT, Sen TK, Ang HM (2012) Equilibrium, kinetics, and thermodynamics of methylene blue adsorption by pine tree leaves. Water Air Soil Pollut 223(8):5267–5282. https://doi.org/10.1007/s11270-012-1277-3

Yan T, Wang L (2013) com adsorptive removal of methylene blue from aqueous solution by spent mushroom substrate: equilibrium, kinetics, and thermodynamics. BioResources 8(3):4722–4734

Zhang J, Zhou Q, Ou L (2012) Kinetic, isotherm, and thermodynamic studies of the adsorption of methyl orange from aqueous solution by chitosan/alumina composite. J Chem Eng Data 57(2):412–419. https://doi.org/10.1021/je2009945

Zhang Z, O'Hara IM, Kent GA, Doherty WOS (2013) Comparative study on adsorption of two cationic dyes by milled sugarcane bagasse. Ind Crops Prod 42(1):41–49. https://doi.org/10.1016/j.indcrop.2012.05.008